Electronic Supplementary Material (ESI) for Journal of Materials Chemistry A.
This journal is © The Royal Society of Chemistry 2016

Facile Synthesis of Hole Transporting Material with Silafluorene Core for Efficient Mesoscopic $CH_3NH_3PbI_3$ Perovskite Solar Cells

Anurag Krishna,[1] Dharani Sabba,[2] Jun Yin,[4] Annalisa Bruno,[2] Liisa J. Antila,[5] Cesare Soci,[4] Subodh Mhaisalkar,[2,3*] Andrew C. Grimsdale[2,3*]

[1]Energy Research Institute, Interdisciplinary Graduate School, Nanyang Technological University, Singapore

[2]Energy Research Institute @ NTU (ERI@N), Research Techno Plaza, X-Frontier Block, Level 5, 50 Nanyang Drive, 637553, Singapore

[3]School of Materials Science and Engineering, Nanyang Technological University, Nanyang Avenue, 639798, Singapore

[4]Division of Physics and Applied Physics and Centre for Disruptive Photonic Technologies, Nanyang Technological University, 21Nanyang Link, Singapore 637371

[5]Department of Chemistry - Angström laboratory, Uppsala University, Regementsvägen 1 75237 Uppsala, Sweden

* Corresponding Authors

1. EXPERIMENTAL SECTION

(a) Synthesis of 4,4'-(5,5-dihexyl-5H-dibenzo[b,d]silole-3,7-diyl)bis(N,N-bis(4-methoxyphenyl)aniline (S101). 3,7-Dibromo-5,5-dihexyl-5H-dibenzo-[b,d]-silole (0.8 g, 1.58 mmol), {4-[bis(4-methoxyphenyl)amino]phenyl} boronic-acid [28] (1.16g g, 3.3 mmol), Pd(0)(PPh3)4 (0.13 g, 0.1 mmol), K_2CO_3 (5 mL) and degassed toluene (20 ml) were transferred in to a 50 mL RBF. This reaction mixture in RBF was then stirred at 90 °C under nitrogen for 48 h. The reaction mixture was cooled down to r.t. and poured into water, extracted with dichloromethane (DCM) and the extract was washed with water. The DCM layer was dried over $MgSO_4$, concentrated and the residue mixture was purified by column chromatography on silica gel eluting with DCM/hexane=1/1 (v/v) to obtain the product as a white solid (0.68 g, 45 %). ^{1}H-NMR ($CDCl_3$, 400MHz): δ(ppm): 7.86 (d, 2H, J=8Hz), 7.80(d, 2H, J=1.6Hz), 7.63 (dd, 2H, J=8.2 Hz), 7.50 (d, 4H, J=8Hz), 7.12 (d, 8H, J=8Hz), 7.04 (d, 4H, J=8Hz), 6.87 (d, 8H, J=8Hz), 3.82 (s, 12H), 1.42 (m, 4H), 1.29 (m, 4H), 1.22 (m, 8H), 0.99 (m, 4H), 0.83 (t, 6H, J=6.8Hz). ^{13}C-NMR ($CDCl_3$, 400MHz): δ (ppm): 155.99, 148.16, 146.79, 141.13, 139.42, 138.71, 133.44, 131.34, 128.46, 127.55, 126.66, 121.17, 121.08, 114.86, 55.65, 33.23, 31.49, 24.08, 22.70, 14.20, 12.56. HRMS (MALDITOF): m/z calcd for $C_{64}H_{68}N_2O_4Si$, 957.34; found, 957.

(b) Device Fabrication

Fluorine doped tin oxide (FTO, <14 ohm/square, 2.2 mm thick) substrates were laser etched to form the desired pattern, which was subsequently cleaned by sonication in decon soap solution and ethanol respectively. A thin compact layer of TiO_2 acting as a blocking layer, is about 80 - 100 nm, was deposited by aerosol spray-pyrolysis, using titanium diisopropoxide bis(acetylacetonate) (75 wt. % in isopropanol) and absolute ethanol in the ratio 1:9 by volume

and ambient air as the carrier gas. Then these substrates were annealed at 450 °C for 30 min and then were treated with 100 mM $TiCl_4$ solution for 60 min at 70 °C, followed by rinsing with deionized water and ethanol and subsequent annealing at 500 °C for an hour. The mesoporous TiO_2 layer composed of 30-nm-sized particles was deposited by spin coating at 5,000 r.p.m. for 30 s using a commercial TiO2 paste (Dyesol DSL 30 NRD) diluted in ethanol (2:7, weight ratio). After drying at 125 °C, the TiO_2 films were gradually heated to 500 °C, baked at this temperature for 15 min and cooled to room temperature. An organic-inorganic perovskite CH3NH3PbI3 was deposited by the published sequential method [3]. Lead (II) iodide (1 M) was dissolved in N,N-dimethylformamide overnight under stirring conditions at 70 ^oC and was spincoated on the substrates at 6000 r.p.m for 5 s. These substrates were then dried for 30 min at 70 °C. Subsequently the films were dipped in 8 mg/mL solution of CH_3NH_3I in 2-propanol for 20 min and were rinsed with 2-propanol and were spun at 4000 rpm for 30s for drying followed by annealing then at 100 °C for 30 min. The HTMs S101 and spiro-OMeTAD were dissolved in chlorobenzene (90 mg/ml and 100 mg/ml) respectively and spincoated on these substrates at 4000 rpm for 30s. Additives like Li $(CF_3SO_2)_2N$, tert-butylpyridine and tris(2-(1H-pyrazol-1-yl)pyridine)cobalt(III) (FK 102) dopant were added to the above solution as per literature [3]. The masked substrates were placed in a thermal evaporator for gold (Au) deposition via shadow masking. Thickness of the Au electrode was about 100 nm and an active area of 0.2 cm^2 was defined by the overlap of TiO_2 and Au.

2. Materials and Equipment

Reactants and reagents, unless otherwise stated, were purchased either from Sigma-Aldrich or Lumtec (Taiwan), and used without further purification. The boronic acid was prepared by a literature route [33]. Both absorption and reflection TiO_2 pastes were purchased from Dyesol.

Column chromatography was carried out using Merck silica (230 – 400 mesh) while thin layer chromatography (TLC) was performed on Merck silica 60 Al-backed plates (20 cm x 20 cm). ^{1}H and ^{13}C NMR data were obtained on a Bruker DPX 400 MHz spectrometer with chemical shifts referenced to DMSO-d_6. Matrix assisted laser desorption/ionization time-of-flight (MALDI-TOF) mass spectra were obtained on a Shimadzu Biotech AXIMA-TOF. UV-Vis absorption spectra were recorded using Shimadzu UV-3600 Spectrometer. CV measurements were carried out on a CHI411 electrochemical workstation. All CV measurements were recorded in CH_2Cl_2 with 0.1 M tetrabutylammonium hexafluorophosphate as supporting electrolyte (scan rate of 100 $mV \bullet s^{-1}$) and the experiments were performed with a conventional three electrodes configuration consisting of a platinum wire working electrode, a gold counter electrode, and an Ag/AgCl in 3 M KCl reference electrode. Photovoltaic measurements utilized an AM 1.5G solar simulator equipped with a 450 W xenon lamp (model 81172, Oriel). Its power output was adjusted to match AM 1.5G sunlight (100 $mWcm^{-2}$) by using a reference Si photodiode. The I–V curves were obtained by applying an external bias to the cell and measuring the generated photocurrent with a Keithley model 2612A digital source meter. The readings were taken in reverse scan mode, with applied potential starting at V_{oc} and being reduced to 0 V. All devices were measured by masking the active area with a black tape mask. Steady-state PL spectra of pure $CH_3NH_3PbI_3$ and $CH_3NH_3PbI_3$/HTM film samples were recorded using a spectrofluorometer (Fluorolog, HORIBA JobinYvon). For time resolved fluorescence spectroscopy, a time-correlated single photon counting (TCSPC) system was used. The samples were excited with a picosecond diode laser (Edinburgh Instruments, EPL405) at 404.6 nm (77.1 ps pulses, 5.5 μW, 1 MHz) and emission was detected after a long pass filter that cut out the scattered excitation light and

covered the entire perovskite emission spectral range. The counts were collected for a 10 min time interval. The TCSPC setup is described in detail in literature [1].

3. COMPUTATIONAL METHODS

The hole transfer can be represented by Marcus-Hush equation of $k_h = \frac{V_h^2}{\hbar}\sqrt{\frac{\pi}{\lambda_h k_B T}} exp\left(-\frac{\lambda_h}{4kT}\right)$, where V_h is the electronic coupling between HOMO levels of neighbouring molecules in the HTM crystals, *T* is the temperature, k_B and $\hbar$ refer to Boltzman and Planck constants. λ_h is the hole reorganization energy calculated by adiabatic potential energy surfaces method. Electronic coupling V_{ij}, defined as $\langle \phi_i \left| \hat{F} \right| \phi_j \rangle$, can be calculated by projecting the Fock Matrix of dimer onto molecular orbitals of respective donor (ϕ_i) and acceptor molecule (ϕ_j) with the subsequent symmetric orthogonalization, where $\hat{F}$ is the Kohn-Sham Fock operator for the dimer system.

Then the hole mobility can be well described by the Einstein relation $\mu = \frac{eD}{k_B T}$, where *e* is the electron charge and *D* is the charge diffusion coefficient of charge carriers, which can be approximately describe as $D = \frac{1}{2d}\sum_i r_i^2 k_i P_i$, where k_i and r_i are the charge-transfer rate and intermolecular distance of the dimer, and P_i is the probability for hole hopping along the *i*th pathway.

The density functional theory (DFT) calculations using CAM-B3LYP functional together with basis sets 6-31G(d, p) were performed to optimize the molecular structures of molecules S101 and spiro-OMeTAD and study their transporting properties. The crystal structures of S101 and spiro-OMeTAD were predicted by using the polymorph module in Material Studio 5.0. The PBE

functional and Dreiding force field were combined to predict the crystal structures. Three possible stable crystal structures with space groups for S101 (C2/C, P/1, and P212121) and Spiro-OMeTAD (C2/C, P21, and P212121) were considered in our study for calculating hole mobility. All the DFT calculations were performed using Gaussian09 program (Revision D.01).

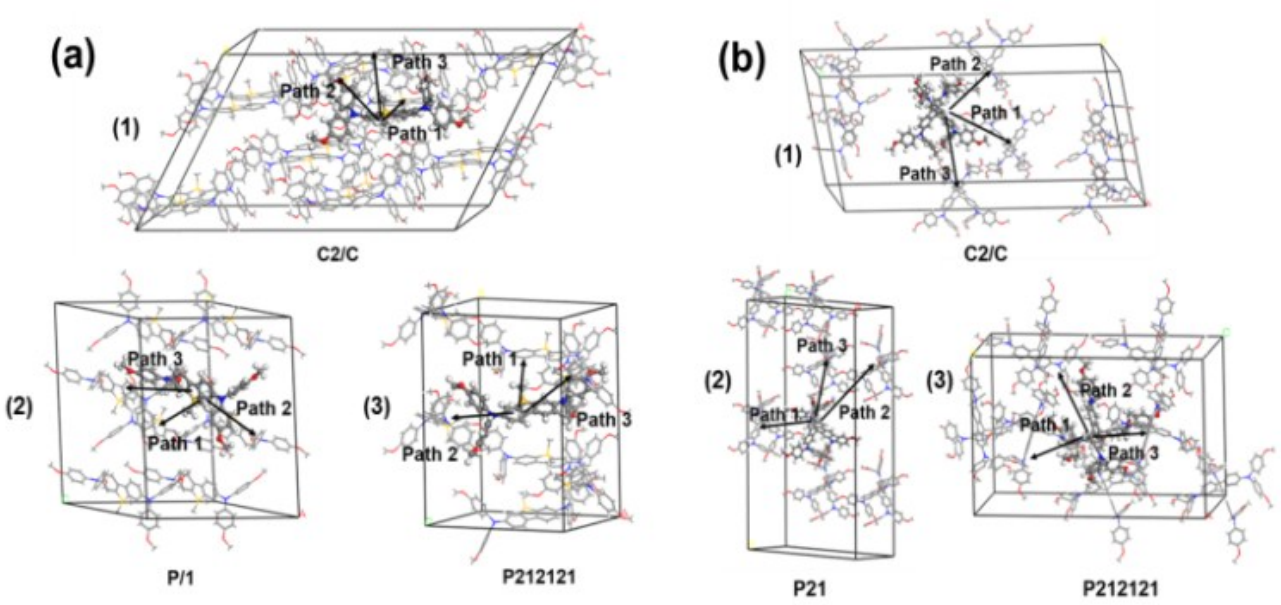

Figure S1. (a) Hole transfer pathways for possible crystal structure (1) C2/C, (2) P/1 and (3) P212121 of S101 molecule; (b) hole transfer pathways for possible crystal structure (1) C2/C, (2) P21 and (3) P212121 of Spiro-OMeTAD molecule.

Table S1. Intermolecular electronic coupling, distance and transfer rate and hole mobility of S101 crystal (Fig 2a).

Crystals	Pathway	Electronic Coupling (meV)	Distance (Å)	Hole Transfer Rate (s^{-1})	Mobility ($cm^2/V{\cdot}s$)
C2/C	1	3.18	8.56750	1.05×10^{11}	0.215
	2	27.5	6.68700	7.81×10^{12}	
	3	5.85	10.86821	3.54×10^{11}	
P/1	1	26.2	5.73052	7.11×10^{12}	0.141
	2	4.91	6.34593	2.49×10^{11}	
	3	5.67	10.81330	3.33×10^{11}	

P212121	1	12.0	7.08085	1.49×10^{12}	0.049
	2	0.25	13.65105	6.50×10^{8}	
	3	0.51	10.72813	2.68×10^{9}	

Table S2. Intermolecular electronic coupling, distance and transfer rate and hole mobility of Spiro-OMeTAD crystal (Fig 2b).

Crystals	**Pathway**	**Electronic Coupling (meV)**	**Distance (Å)**	**Hole Transfer Rate (s^{-1})**	**Mobility ($cm^2/V\cdot s$)**
C2/C	1	1.13	17.15	1.32×10^{10}	0.0058
	2	1.99	15.24	4.10×10^{10}	
	3	1.96	16.00	3.96×10^{10}	
P21	1	0.95	16.02	9.38×10^{9}	0.0046
	2	2.08	13.67	4.48×10^{10}	
	3	0.45	16.30	2.14×10^{9}	
P212121	1	2.67	15.52	7.36×10^{10}	0.0532
	2	7.80	11.92	6.30×10^{11}	
	3	0.11	14.88	1.26×10^{8}	

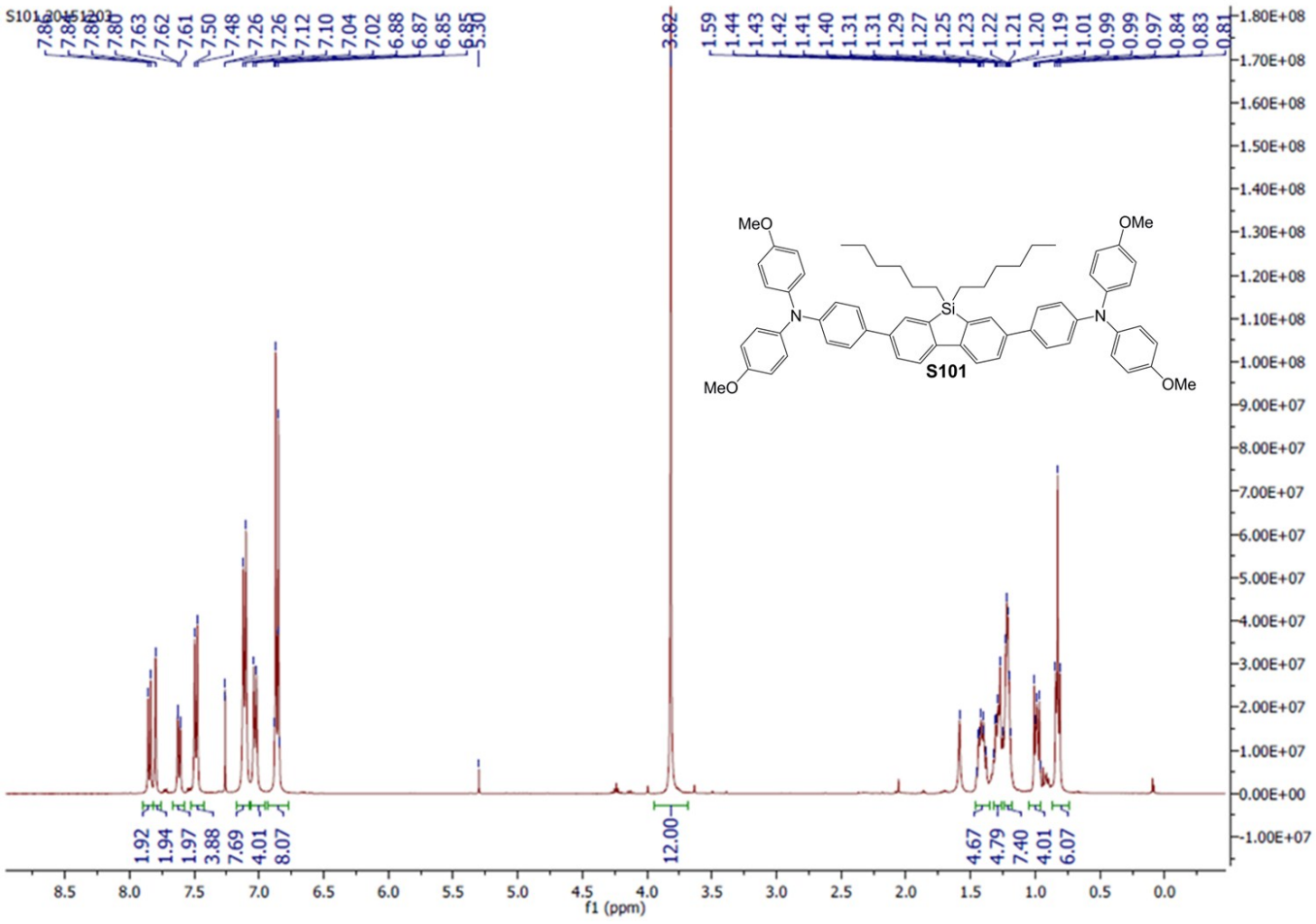

Figure S2. ^{1}H NMR spectrum of S101.

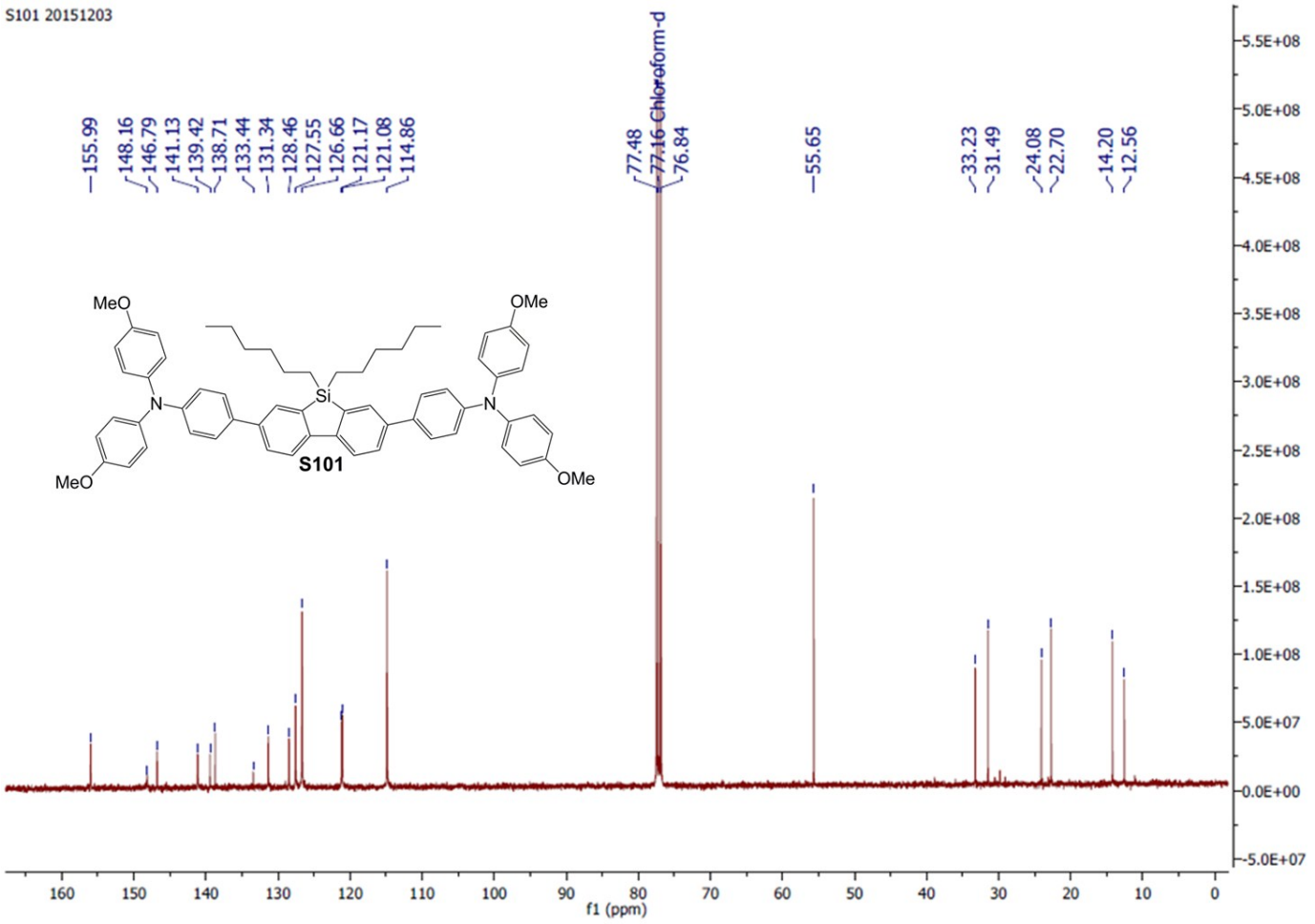

Figure S3. ^{13}C NMR spectrum of S101.

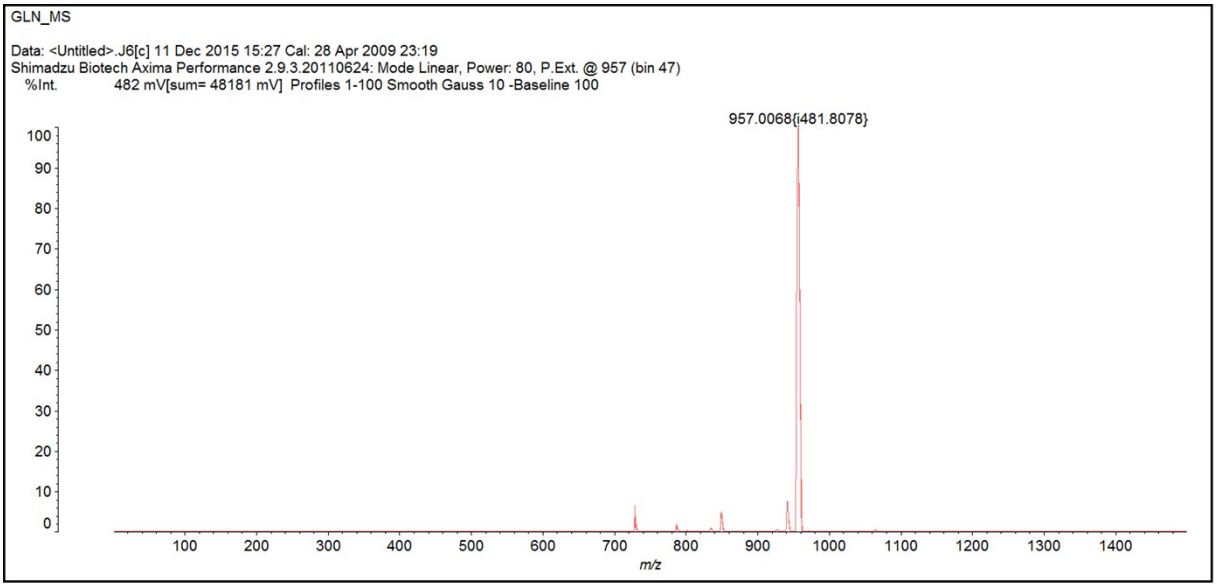

Figure S4. MALDI-TOF mass spectra of S101.

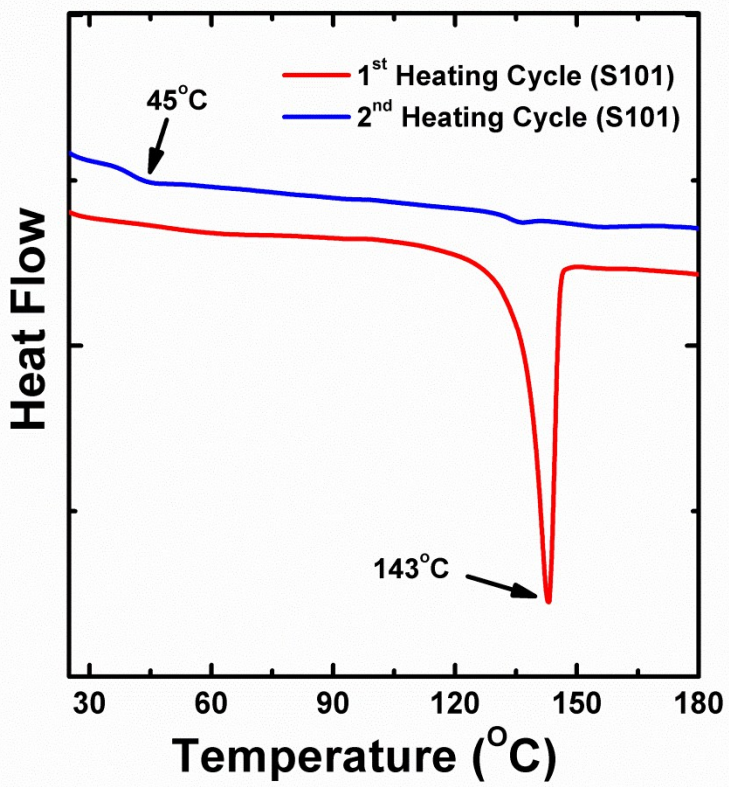

Figure S5. Differential Scanning Calorimetry (DSC) curves for S101.

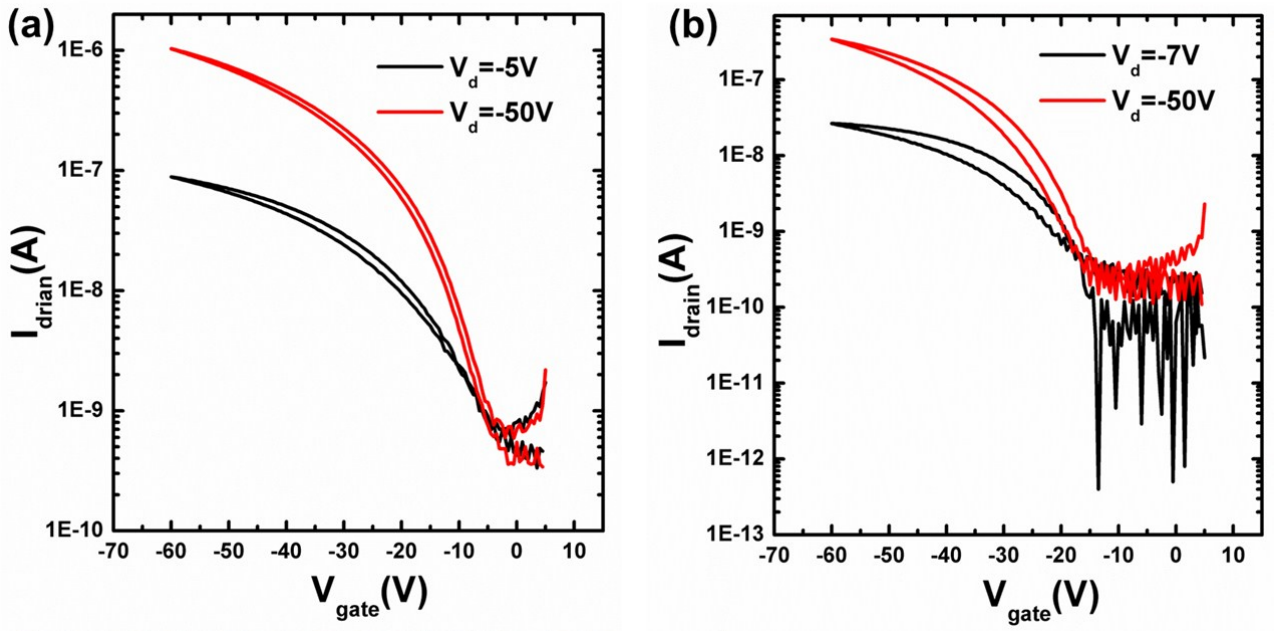

Figure S6. Transfer characteristics in the p-channel type FET of (a) spiro-OMeTAD and (b) S101. These characteristics are measured at V_g= -40V.

Table S3. Time resolved photoluminescence characterization of the $CH_3NH_3PbI_3$ perovskite.

	Fraction	τ_1 (ns)	Fraction	τ_2 (ns)	τ_{av} (ns)
$CH_3NH_3PbI_3$	0.65	3.5	0.35	1.2	2.7
$CH_3NH_3PbI_3$/Spiro	0.64	0.78	0.36	0.71	0.8
$CH_3NH_3PbI_3$/S101	0.62	1.02	0.38	1.1	1.1

Analysis of relative costs of manufacture of spiro-OMeTAD and S101

The detailed comparisons between the synthesis of Silole based HTM and spiro-OMeTAD are discussed here, in terms of number of steps, yields of each step, cost of starting materials and total reaction time. As shown in the **Scheme S1**, the comparisons are actually focused on the

synthesis of tetrabromo-spirofluorene core (compound **6**) and S101 core 3,7-(dibromo-5,5-dihexyl-5H-dibenzo[b,d]silole) (compound **12**). The data is summarized in **Table S4**.

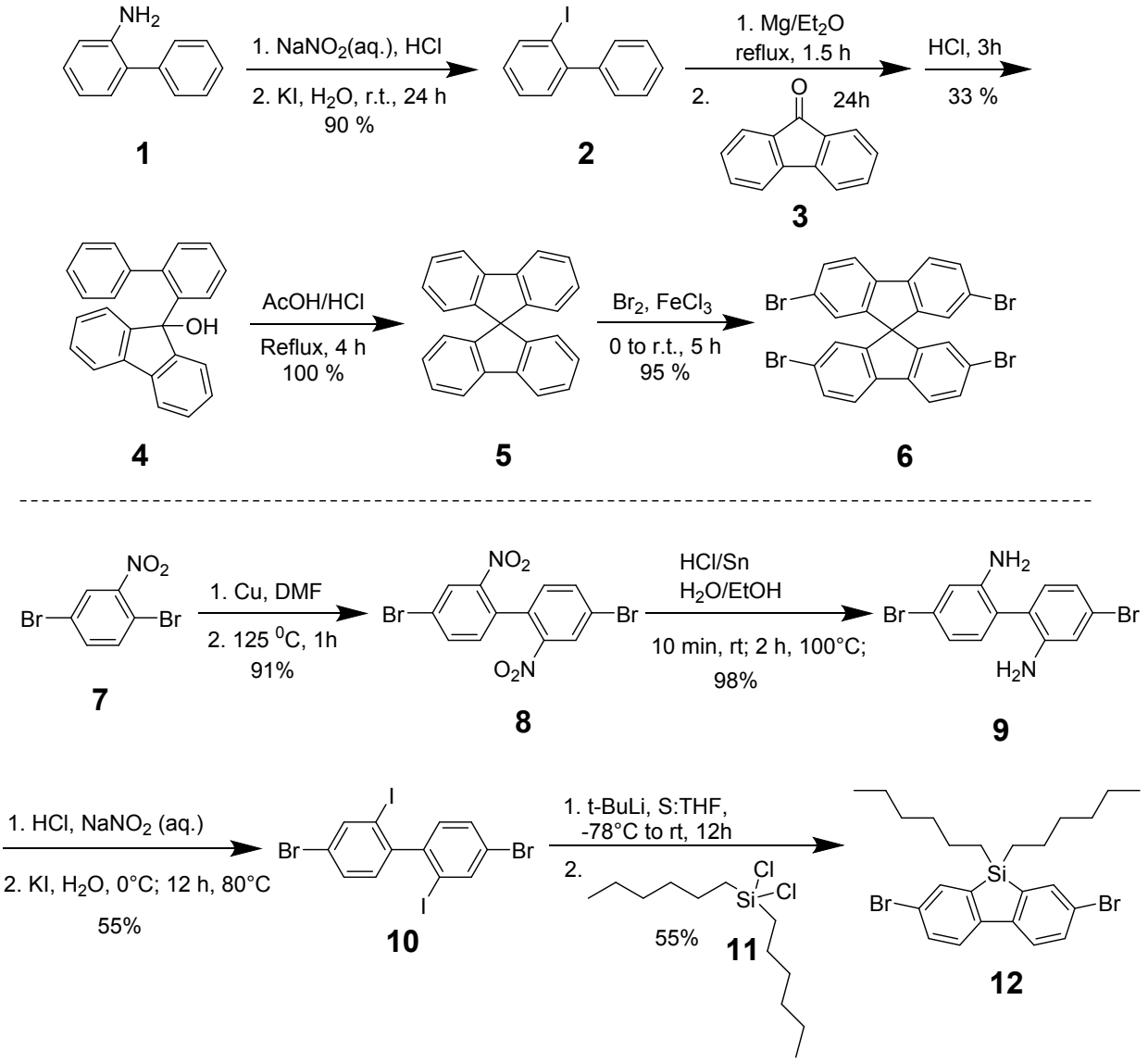

Scheme S1. Synthetic schemes to the core **6** and **12**, with reaction condition, duration of time and yield of each step indicated.

First of all, in both cases four steps are needed to achieve core molecules from readily available and cheap starting materials. Moreover, the equal number of steps makes the comparison easier. The prices were quoted from Alfa Aesar US website and Fluorochem UK with the largest

possible package size available for fair comparison. The costs of solvents and reagents used in both routes such as THF, DMF, acids, salts, etc. were assumed to be approximately the same - these are very common and inexpensive chemicals and there is an equal number of steps.

In order to make 10 g of (spiro) core **6**, the amount of compound **1** and **3** consumed, calculated from the yield of each step, is 9.0 g and 9.1 g, respectively. The unit price of compound **1** and **3**, is \$76.3/5g and \$580/2.5kg, respectively. As a result, the total cost of starting materials for making core **6** is \$139.5/10g. For comparison, the price of spiro-OMeTAD from Merck, one of the few licensed companies, is about \$850/g. In the same way, in order to make 10 g of (S101) core **12**, the amount of compound **7** and **11** consumed, calculated from the yield of each step, is 20.7 g and 9.3 g, respectively. The unit price of compound **7** and **11**, is \$135.9/100g and \$271/50g, respectively. As a result, the total cost of starting materials for making core **12** ~ \$76/10g. The difference will be rather considerable when scaled up.

The total duration time of the reactions from first step to the end is an important factor to estimate the timeline for production. As we can see from **Table S1** that the total reaction time for making core **12** is almost half of the amount of time for making core **6**. Since both have four steps, it can easily conclude that it is faster to make core **12** than core **6**, which not only saves the time but also saves the manpower which is much more expensive.

In short, we can confirm that making core **12** is cheaper than core **6**. In addition the purification of spiro-OMeTAD requires expensive sublimation, whereas S101 can be purified by cheaper methods such as column chromatography.

Table S4. Summarization of the comparisons, the better one is highlighted.

	total cost of starting materials	number of steps	total duration of reactions	estimated number of days to complete the process
Core **6**	\$139.5/10g	4	59.5 hours	5 days
Core **12**	\$76/10g	4	27 hours	3 days

References

1. A. El-Zohry, A. Orthaber and B. Zietz, *J. Phys. Chem. C,* 2012, **116 (50)**, 26144-26153.